www.amlett.com, DOI: 10.5185/amlett.2010.5124 Published online by the VBRI press in 2010

pH dependant fungal proteins in the 'green' synthesis of gold nanoparticles

Rashmi Sanghi*,†, Preeti Verma

302 Southern Laboratories, Facility for Ecological and Analytical Testing,

Indian Institute of Technology Kanpur, Kanpur 208016, India

*Corresponding author. Tel: (+91) 512 2597844; Fax: (+91) 512 2597866; E-mail: rsanghi@gmail.com

†Present address. The LNM Institute of Information Technology, Jaipur, Post-Sumel, Via-Jamdoli, Jaipur 302031, India.

Received: 18 May 2010, Revised: 2 July 2010 and Accepted: 8 July 2010

ABSTRACT

An efficient, simple and environment friendly biosynthesis of gold nanoparticles (GNPs), mediated by fungal proteins of *Coriolus versicolor* is reported. By altering the reaction conditions, the intracellular synthesis of GNPs on the fungal mycelium, could be well tailored to produce extracellular GNPs in the aqueous medium. The reaction rate and the morphology of the particles were found to depend on parameters such as pH, incubation temperature and concentration of gold solution. The gold nanoparticles were characterized by UV–Vis, SEM and AFM techniques, demonstrating high stability of gold nanoparticles in aqueous media, *via* the protein layer. The size of the gold nanoparticles using AFM studies was found to be in the range 5–30 nm. These nanoparticles were found to be highly stable as even after prolonged storage for over 6 months they do not show aggregation. A plausible mechanism explaining the role of different possible proteins under different conditions, in the formation of gold nanoparticles has been investigated using FTIR. This study represents an important advancement in the use of fungal protein for the extracellular synthesis of functional gold nanoparticles by a green and mild technique in one pot.

Keywords: Gold; nanoparticles; fungus; protein.

Rashmi Sanghi is currently working as a Research Scientist at The LNM Institute of Information Technology, Jaipur, India. She obtained her D. Phil. degree from Chemistry Department, University of Allahabad, India in 1994. Ever since, she worked at the Indian Institute of Technology, Kanpur, India as Research Scientist till 2008. Her major research interests are environmental green chemistry with focus on microbial and nanoparticle research.

Preeti Verma obtained master degree in Biotechnology from Institute of Biological Science and Biotechnology, CSJM University, Kanpur, India in 2006. Her research work is on the biosynthesis and characterization of nanoparticles, and bioremediation of heavy metals. She is going to defend thesis very soon.

Introduction

Synthesis of nanoparticles has great interest due to their unusual optical [**1**], chemical [**2**], photoelectrochemical [**3**], and electronic [**4**] properties. In the area of nanotechnology, the development of techniques for the controlled synthesis of metal nanoparticles of well-defined size, shape and composition is a big challenge. Various chemical and physical synthesis methods, aimed at controlling the physical properties of the particles, are currently employed in the production of metal nanoparticles. Most of these methods are still in the development stage and problems are often experienced with stability of the nanoparticle preparations, control of the crystal growth and aggregation of the particles [**5**]. The synthesis and assembly of nanoparticles would benefit from the development of clean, nontoxic and environmentally acceptable ''green chemistry'' procedures, probably involving organisms ranging from bacteria to fungi and even plants [**6**]. Hence, both unicellular and multicellular organisms are known to produce inorganic materials either intra or extracellularly [**7**]. Using metal-accumulating microorganisms as a tool for the production of nanoparticles, and their assembly for the construction of new advanced materials, is a completely

new technological approach. The common Lactobacillus strains found in buttermilk was used for the formation of gold, silver, and gold-silver alloy crystals [**8**]. Recently, bacterial cell supernatant of *Pseudomonas aeruginosa* was used for the reduction of gold ions resulting in extracellular biosynthesis of gold nanoparticles [**9**]. The extremophilic actinomycete, *Thermomonospora sp.* when exposed to gold ions reduced the metal ions extracellularly, yielding gold nanoparticles with a much improved polydispersity [**10**]. Endophytic fungus *Colletotrichum sp.* growing in the leaves of geranium was used for the extracellular synthesis of stable and various shaped gold nanoparticles. Reducing agent in this fungus were also polypeptides/enzymes [**11**]. The self-organization of monolayers of colloidal gold nanoparticles on fungal mycelia grown from spores of *Aspergillus niger*, which were added to the colloidal solution has been reported earlier [**12**]. Living filamentous fungi has been also used for the formation of colloidal gold nanoparticles [**13**]. The synthesis of gold NPs at room temperature by reduction of gold ions using Rhizopus oryzae [**14**] and the intracellular formation of gold nanoparticles using the fungus *Verticillium sp*. was also reported [**15**]. Recently the extracellular synthesis of gold nanoparticles by treatment of the fungus *Fusarium oxysporum* with aqueous $AuCl^{4-}$ ions has also been reported [**16**].

For Gold nanoparticles used for biological application, the introduction of active groups, such as -NH_2, -COOH and -SH on GNPs is an important aspect. If the amino acid molecules could be directly fixed on GNPs during the synthesis of GNPs, it can be very useful and convenient in biological applications. So, in this work, we have focused on the use of fungi for both intra- and extracellular synthesis of protein capped gold nanoparticles by optimizing the parameters so as to minimize the time and maximize the yield. Also, the role of different proteins under different conditions was evaluated. Studies were carried out both with the native fungus as well as the growth media in which the fungus was grown so as to monitor the intra/extracellular formation of Au NPs.

Experimental

Growth of the fungus

The white rot fungal strain *Coriolus versicolor* was obtained from Institute of Microbial Technology (IMTECH), Chandigarh, India. The strain was maintained at 4 °C on malt agar slants. Erlenmeyer flasks of the capacity 150 mL was used for growing the fungal mycelia. It contained 50 mL of the growth medium, consisting of 5 g/L Malt Extract Powder and 10 g/L glucose. The medium was autoclaved ('WidWo' Cat. AVD 500 'horizontal autoclave') at 15 psi for 30 min and cooled to room temperature before use and the pH after autoclaving was 5.6.

All the chemicals used were of analytical grade. The media components like glucose, Malt extract powder were obtained from S.D. Fine Chemicals, Mumbai, India.

Methods

Experiments were conducted with the fungal mycelium as well as with the growth media in which the fungus was grown and harvested for 7 days. These two sets of experiments were conducted at normal pH (2.0 - 3.5) and 37 °C with constant shaking at 200 rpm in an incubator shaker (normal conditions).The effect of concentration of glucose on culture media, pH, temperature, time, and concentration of gold solution (0.5 mM, 1mM and 2 mM) was studied by varying one parameter at a time, keeping the other experimental conditions the same. The experiments were conducted at alkaline conditions at room temperature without stirring.

Typically around 4-5 gm of fungal mycelium (fresh wet weight) or 30 mL of the neat growth media was brought in contact with 0.5mM concentration of $HAuCl_4$ in a 150 mL Erlenmeyer flask and agitated at 37 °C (normal conditions) at 200 rpm. Simultaneously, a positive control of incubating the fungus mycelium with deionized water and a negative control containing only gold solution were maintained under same conditions. Sample of 1mL was withdrawn at different time intervals and the absorbance was measured at a resolution of 1 nm using UV–visible spectrophotometer (UV–Vis). The mechanistic details were further worked out by various instrumental analyses. The gold nanoparticles thus formed were subjected to different analytical techniques to characterize them.

Characterizations

For the measurement of the UV–Vis absorbance, were recorded with a UV/Vis, Spectrophotometer Lambda 40, (Perkin Elmer, USA) in the wavelength range of 200–800 nm. The deionized water was used as the blank. Infrared (IR) spectra were recorded on a BRUCKER, VERTEX -70, Infrared spectrophotometer making KBr pellets in reflectance mode. The composition of gold nanoparticles was studied by the method of x-ray diffraction analysis on a recorded in ARL X′ TRA X-ray Diffractometer and the x-ray diffracted intensities were recorded from 10° to 80° 2θ angles. For the observations of Scanning electron micrographs SEM, the powered gold nanoparticles were mounted on specimen stubs with double-sided adhesive tape and examined under FEI (QUANTA 200) SEM at 10–17.5 kV with a tilt angle of 45°. Their corresponding EDX spectrum was recorded by focusing on a cluster of particles. We have also imaged protein capped gold nanoparticles on mica substrate using an atomic force microscope (AFM). Samples for AFM imaging were prepared by a drop of aqueous solution containing the gold nanoparticles was placed on the mica film and then dried under room temperature. Atomic force microscopy (AFM) images were obtained using a Picoscan TM Molecular imaging, USA.

Results and discussion

The washed fungal mycelium and the growth medium in which the fungus was harvested were separately challenged with 0.5 mM of $HAuCl_4$ solution and incubated in shaker (200 rpm) at 37 °C (normal conditions). The pH of the solution was 3.5. After exposure to aqueous solution of $HAuCl_4$ with the fungal mycelium, the fungal mycelium turned vivid purple after 6h indicating the intracellular formation of Au nanoparticles. The aqueous Au-growth medium remained colorless and showed no discernible absorption in the 500-600 nm regions even after two days

indicating that extracellular reduction of $AuCl_4^-$ ions has not occurred [**17**]. In case of growth media reduction of gold ion has not occurred under normal pH.

The presence of glucose in the growth media is vital for the enhancement of protein release which in turn is related to the reduction of GNPs. It was observed that the protein release increased with the increase in glucose concentration. So, studies were conducted with optimized glucose concentration which was found to be 10 g/L (data not shown). Under normal conditions wherein the pH was 3.5, reduction of gold ion occurred within 6 hrs and was intracellular with experiments with fungal mycelium. According to the hard soft acid base theory (HSAB) oxygen is a hard base and gold is a soft acid, therefore the interaction between these two elements is presumably low but the interaction of gold (III) with a nitrogen or sulfur groups (soft base) should be reasonably higher [**18**]. So the intracellular reduction of gold ions shows the pH dependency for the binding of trace levels of $AuCl_4^-$ to the fungal mycelium. At low pH the carboxyl group is protonated and neutrally charged, therefore the repulsion of negatively charged $AuCl_4^-$ ions should decrease with decreasing pH and thus allow for higher gold (III) binding. Furthermore, amino groups carry more positive charge at lower pH, thus enhancing the binding of $AuCl_4^-$ ions at reduced pH. The maximum binding of the gold ions to the fungal mycelium occurred at pH 2-3 and decreased almost linearly with increase in pH.

At low pH no extracellular production of GNPs was observed in the case of growth media as well as mycelium, even with the high release of proteins. Whereas under alkaline conditions (pH 11), the color changes with time from colorless to wine red with increasing intensity, indicated the formation of gold nanoparticles extracellular in both case whereas intracellular synthesis was not observed in case of Au/ fungal mycelium. This differential behavior of proteins is because some proteins are highly active only at alkaline pH.

Extracellular synthesis offers a great advantage over an intra-cellular process of synthesis from the application point of view. The surface trapped nanoparticles or those formed inside the biomass would require an additional step of processing like ultrasonication for their release into the surrounding liquid media. The intracellularly produced nanoparticles are sonicated in a bath sonicator at 60 °C for 30 min in 1M NaOH (5 mL) resulting in the partial solubilisation of the particles and formation of a vivid purple solution [**19**].

Fig. 1 shows the UV–Vis absorption spectra from the resulting solutions synthesized by reduction of gold solution with fungal mycelium at normal pH as well as spectra of Au/mycelium and Au/media at pH 11. UV–visible spectrum of the solutions was recorded to study the change in light absorption profile of the medium. Most of the interesting observations made were studied under the two ranges 200-300 nm and 350-600 nm.

It is reported earlier that proteins can bind to nanoparticles either through free amine groups or cysteine residues in the proteins and via the electrostatic attraction of negatively charged carboxylate groups in enzymes present in the cell wall of mycelia and therefore, stabilization of the gold nanoparticles by protein is a possibility [**20**]. In the beginning of the reaction, the absorption spectrum showed a peak at around 280 nm indicating the presence of aromatic residues in the proteins. This could be arising due to the π–π^* transition in the indole part of the molecule of tryptophan and tyrosine residues of the proteins present in the solution [**21**]. The absorbance at 280 nm maintained the same intensity throughout the incubation time under normal pH conditions with mycelium indicating that these proteins have no role to play in the intracellular formation of GNPs.

With increase in pH to 11, both in mycelium and as well as in media experiments, the hump at 280 disappeared showing the significant role played by the aromatic amino acids tryptophan and tyrosine in gold ion reduction. Tyrosine [**22**] and tryptophan [**23**] are known to act as pH dependent reducing agent under alkaline conditions, but not under neutral or acidic conditions to yield highly stable GNPs. The reducing ability of tyrosine at alkaline pH is due to the ionization of the phenolic group in the amino acid to phenolate ions, which thereafter reduce the gold ions, by electron transfer, into gold nanoparticles. So the simultaneous mixing of the tetrachloroauric acid and with mycelium as well as with media results in the rapid formation of stable gold sols as indicated by the appearance of the win red color. It was observed that as the reaction proceeds and gold nanoparticles are formed, the absorption wavelength of the π–π^* transition shifts from 280 nm to 260 nm at initial phase of reaction. This blue shift is a strong indication of either coordination of the tryptophan or tyrosine molecules with the surface of the gold nanoparticles or a reaction leading to a more drastic change in the electronic structure of the amino acid [**22**].

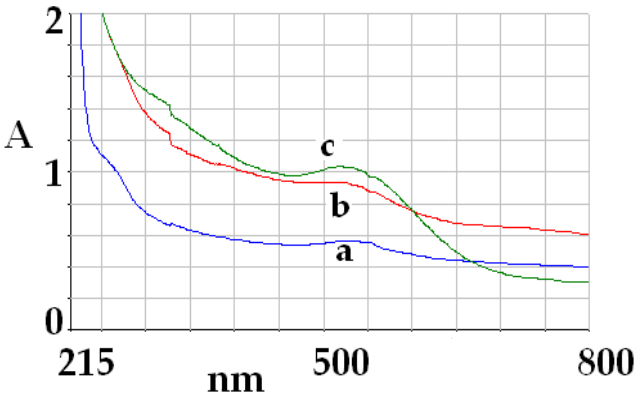

Fig. 1. UV–Vis spectra of the (a) Au/mycelium at normal pH (b) Au/mycelium at pH 11 (c) Au/media at pH 11.

UV-Vis absorption measurements in the range 350-600 nm can provide a deeper insight into the optical properties of the formed nanosized Au particles, and provide information about their size, size distribution, and surface properties. The characteristic surface plasmon (SP) resonance band of Au nanoparticles is centered at about 520 nm [**24**]. In the current study, under normal pH conditions, the characteristic SP absorption band at 528 nm (2.34 eV) was observed after 6 h in case of fungal mycelium, whereas at pH 11, the absorbance band was blue shifted to 518 nm shifting slightly to high energy (2.39 eV) indicating decreased particle size in Au/fungal mycelium

solution respect to normal conditions. In case of media at pH 11, the absorbance band at 527 nm was blue shifted to 518 nm (2.39 eV) with increasing time indicating decreased particle (**Fig. 2**). When the pH was increased to 11, the time taken was reduced to only 5min in case of media and 3 h with mycelium as monitored by progressive enhancement in intensity (**Fig. 2**) of the SP band of Au nanoparticles, indicating the increased yield and the high absorbance features [**25**].

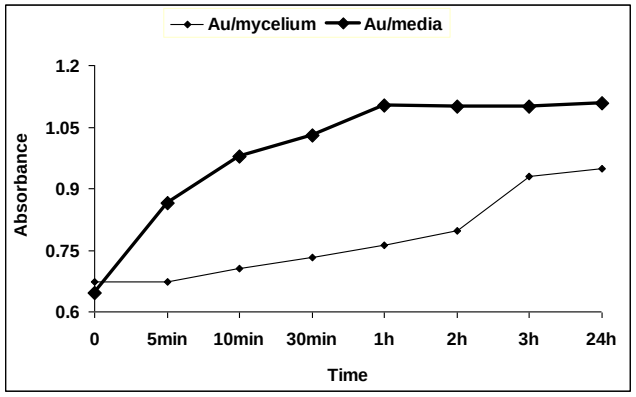

Fig. 2. Increase of absorbance intensity with time at pH 11.

The increase in the concentration of the gold solution causes an acceleration of the reduction reactions in the homogeneous phase as confirmed by the shortening of the induction period that precedes the nucleation of gold to 3 hrs under normal conditions only in the case of fungal mycelium experiment. With the increase in concentration of the reacting gold solutions, not much change was observed in the size of the resulting gold nano particles as evident by AFM.

It is generally believed that the reaction temperature will have a great effect on the rate and shape of particle formation. The rate of formation of the nanoparticles was related to the incubation temperature and increased temperature levels allowed particle growth at a faster rate. With increase in temp the time taken for the GNPs formation was much reduced. At a lower temperature (20 °C), the majority of nanoparticles formed after 72 h which reduced to 10hrs at 28 °C whereas exposure to gold solution at higher temp (37 °C) takes less than six hour. The results indicate that, with the reaction temperature increasing in the range 20–37 °C, the maximum absorption wavelengths of gold colloids take on a blue shift (from 543 to 528 nm), showing a decreasing tendency for the size of gold nanoparticles.

Characterization of gold nanoparticles

X-ray diffraction studies

Further evidence for the formation of gold nanoparticles is provided by X-ray diffraction (XRD) analysis of the Au nanoparticles formed with fungal mycelium experiments. A strong diffraction peak at 38.6° was ascribed to the fcc gold structures, while diffraction peaks of other four facets were much weaker (**Fig. 3**). The four strong Bragg diffraction peaks at 38.6°, 44.3°, 64.6°, and 77.35° closely matched that of gold [**26**]. As expected, the XRD peaks of the nanoparticles were considerably broadened because of the finite size of the nanoparticles.

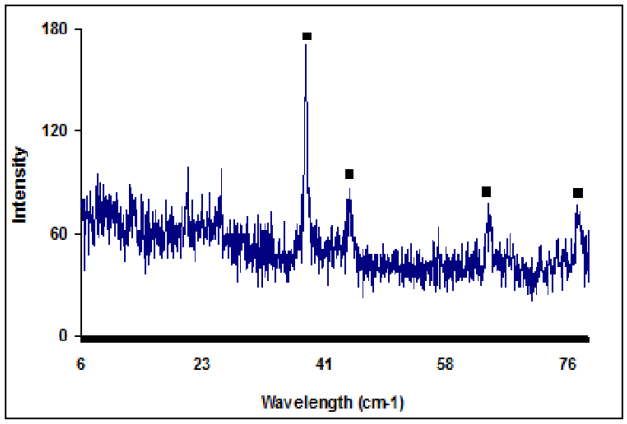

Fig. 3. X-ray diffraction pattern of Au/fungal mycelium, filled square (●) indicate the peaks corresponding to that gold nanoparticles.

Fourier transform infrared spectroscopy

FTIR measurements (**Fig. 4**) were carried out to identify the possible interactions between gold ions and fungal proteins which act as reducing agent to synthesize and stabilized gold nanoparticles due to its containing three main functional groups, including the amino, carboxylic, and thiol group, which are easily used as active sites to modify the other molecules or nanomaterials.

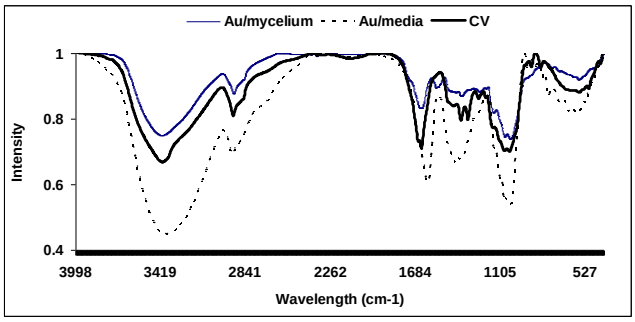

Fig. 4. FT-IR of plain fungus (CV), CV-Au/media and CV-Au/mycelium.

The broad band contour which appears in the range of 3000–3400 cm^{-1} is the summation of association intermolecular hydrogen bonds arising from -NH_2 and -OH groups in protein molecules which becomes much broader after the reaction with gold ions both in Au/mycelium as well as Au/media. The significant change of transmittance related to the bonds with nitrogen atoms reveal that nitrogen atoms are the binding sites for gold on fungus which further broadens and becomes symmetrical, indicates that the N-H vibration was affected due to the gold attachment.

The two bands observed at 1367 cm^{-1} and 1029 cm^{-1} can be assigned to the C–N stretching vibrations of aromatic and aliphatic amines, respectively. The aromatic amine band becomes much intensified in the case of media at alkaline pH but not in fungal mycelium at normal pH. Infrared active modes attributed to side chain vibrations include C-H stretching anti-symmetric and symmetric modes at 2917 cm^{-1} and 2850 cm^{-1} corresponding to

aliphatic and aromatic modes respectively broaden after the reaction with gold solution in case of mycelium at normal pH and becomes disappear in case of media at alkaline pH. The band at ca. 1465 cm^{-1} is assigned to methylene scissoring vibrations from the proteins in the solution. With alkaline pH the significant changes observed for peaks at 1367 cm^{-1}, and 2850 cm^{-1} is indicative of the role of aromatic groups in reduction of Au ions in Au/media which possibly arise from aromatic amino acids tryptophan or tyrosine as discussed above.

It is notable that a new band at about 1735 cm^{-1} (**Fig. 4**) corresponding to carbonyl stretch vibrations in ketones, aldehydes and carboxylic acids indicating that the reduction of the gold ions is coupled to the oxidation of the hydroxyl groups and/or its hydrolyzates, which may be attributed to the formation of a quinone structure due to the oxidation of the phenolic group of aromatic amino acids.

The most useful IR band for the direct measurement of secondary structure of protein is a broad band found between 1652 cm^{-1} and 1637 cm^{-1}. The amide 1 band is primarily a C-O stretching mode arising almost exclusively from the C-O vibration of the peptide linkages of the protein chain [**27**]. The maximum absorbance of the amide 1 band of proteins with predominantly alpha helix structure were found in pure fungal mycelium samples near at 1652 cm^{-1} and those with predominantly beta sheet structure at 1637 cm^{-1}. After the reaction, the amide I peak appeared as a single peak at 1637 cm^{-1} under normal pH conditions with Au/ mycelium. The peaks at 1637 cm^{-1} and 1151 cm^{-1} arise from a carbonyl stretching vibration and phenolic groups of tyrosine and tryptophan, respectively, which shows the carbonyl stretching vibration from the carboxylate ions and the hydroxyl stretching vibration from the phenolic ions in Tyr of the pure fungus [**22**]. This indicated that the secondary structure of the proteins is affected as a consequence of reaction with the Au ions or binding with the gold nanoparticles.

The strong absorption band at 2105 cm^{-1}, 2160 cm^{-1} and 2190 cm^{-1} associated with the isonitrile in pure fungal mycelium was absent in gold nanoparticles indicating the strong role of -N≡C group in gold nanoparticles synthesis [**28**]. Isonitriles are effective in causing condensation of amino acids having masked amino groups with compounds having active hydroxyl groups to the corresponding amino acid esters. The compounds having active hydroxyl groups that may be combined with N-protected amino acids in the presence of an isonitrile to form esters are a broad class [**29**]. The masked amide II band is a combination of N-H in plane bending and C-N stretching was clearly observed in gold nanoparticles at 1544 cm^{-1} in both cases. A shift of ν cm^{-1} ±3 is also seen in the more complex Amide III band located near 1243 cm^{-1} in fungal mycelium as well as in media. The sharp and intense peaks, which also arise due to various interactions of the proteins group and Au ions, appear at around 848 cm^{-1}, 887 cm^{-1}.

Some very interesting observations were made after the reaction. Peaks which could be ascribed to the presence of proteins arise after the reaction with fungal mycelium (normal pH) as well as the Au/media (alkaline pH). An aromatic C-C stretch at 1151 cm^{-1} and a C-H bend at 837 cm^{-1} could be well assigned to the aromatic residue tyrosine and the C-H bending mode of the aromatic residue tryptophan detected at 752 cm^{-1}. Apart from this the spectrum also shows peaks at 600 cm^{-1}, 665 cm^{-1} and 715 cm^{-1} due to C-S stretching; these C-S stretching modes of the sulfur-bearing residues confirm the presence of cysteine and methionine. Additionally C-S stretching modes from the sulfur-bearing residues of cysteine and methionine were detected at 626 cm^{-1} and 642 cm^{-1}. The peaks at around 1151 cm^{-1}, 1097 cm^{-1}, 1074 cm^{-1} in the n–C–O stretching vibration region, is indicative of gold ions interaction with the fungal protein of mycelium as well as media.

FT-IR also yields the information regarding composition of "thiol derivatives" surrounding the metallic cores. The ν SH stretches occur at 2590–2500 cm^{-1} and was clearly seen in the plain mycelium. After the reaction, at normal pH, the absorption peak at 2538 cm^{-1} associated with the –SH stretch vibration that are present in the cysteine residues in the enzyme [**30**] completely disappears from the mycelium. The disappearance of the ν SH stretching band indicates the formation of a bond between the S atoms and gold clusters. It indicates chemisorption on gold surface as thiolate by forming an Au-S bond. A broad feature at about 2547 cm^{-1} in case of media at alkaline pH arises due to the free/ uncoordinated-SH stretching vibrations indicating that these infrared modes are conserved in Au/media, this confirms that the side- chain thiol functional groups, which are critical in determining the bioactivity of the protein, remain intact after nanoparticle conjugation occurs. Whereas in Au/mycelium the peptide backbone does not remain intact after nanoparticle conjugation has occurred. It clearly indicates that at alkaline pH SH group does not play role in gold ion reduction.

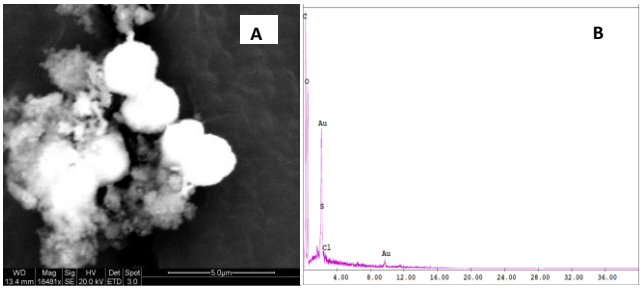

Fig. 5. (A) SEM image of gold nanoparticles (B) EDAX Spectrum of gold nanoparticles.

Scanning electron microscopy

The presence of mycelia covered with well-dispersed gold nanoparticles can be observed by scanning electron microscopy (**Fig. 5A**). The gold nanoparticles appear to be on the surface of the mycelia. Aspot-profile energy-dispersive analysis of X-rays (EDAX) of one of the gold nanoparticles shows the presence of strong signals from the gold atoms together with weaker signals from C, O, S and Cl atoms (**Fig. 5B**). The C and O signals arise from X-ray emission from proteins/enzymes either directly bound to the gold nanoparticle or in the vicinity of the particle, while the presence of a weak Cl signal indicates the presence of a small fraction of $AuCl_4^-$ ions in the region being investigated.

Atomic force microscopy

AFM study was carried out to investigate any morphology change in formed gold nanoparticles that occurs from Au/ fungal mycelium as well as Au/media under alkaline conditions at pH 11. Clearly, the particles are much denser, closely packed, uniformly ordered layered and spherical or elliptical in shape in case of Au/mycelium (**Fig. 6**). The shape of the formed gold nanoparticles is spherical and elliptical in both cases. The particle size of the NPs is in the range of 20-100 nm in Au/media and 100-300 nm in Au/mycelium. The particle size of extracellularly formed nanoparticles of Au/media is much lesser as compare to intracellularly formed Au/mycelium which could be due to the role of different protein in gold reduction. Different morphologies (spheres or elliptical) were observed on different parts of the cell walls possibly because the distribution of functional proteins on the cell walls was not uniform.

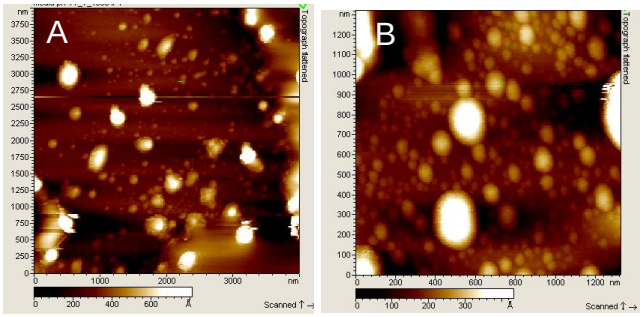

Fig. 6. AFM of Au/fungus solution at pH 11. A and B are Au/media and Au/mycelium, respectively.

Mechanism

The possible mechanism for gold nanoparticle formation on the cell walls of fungal biomass can be explained as below. Gold ions were first trapped and reduced by the proteins on the cell surface at normal pH (2.0 - 3.5), forming nuclei, followed by extensive crystal growth into the final shapes. The positive amino and sulfhydryl (SH) groups of fungal protein at low pH makes Au (III) available for the binding and allow the reduction of Au (III) to Au (0). Carboxylic groups, which are abundant in biomass, are known to be protonated at low pH also contribute to the binding of Au (III) ions [**31**]. These groups of the biomass might carry more positive charge at low pH values, which weakens the reducing power of the biomass and allows the $AuCl_4^-$ ions to get closer to the binding sites thus allowing the subsequent formation of larger amounts of nanoparticles with smaller diameters. The fact that the resulting gold nanoparticles prepared by this method are stable for very long periods of time in spite of the absence of any additives indicates that the particles are electrostatically stabilized. These results show that the starting pH could have an important effect on the size and shape of gold nanoparticles. In case of media synthesis of gold nanoparticles does not occur at low pH, whereas increase in pH, extracellularly synthesis of gold nanoparticles takes place. So on increasing pH values, the reducing power and reaction rate increase correspondingly and could contribute to the formation of thermodynamic favored spherical particles [**27**]. Thus, different pH would be regulated the proton concentration resulting in the control of gold nanoparticles morphology.

Conclusion

We have shown that gold nanoparticles formed by fungal protein of carbon. versicolor under different experimental conditions. The rate of nanoparticles formation and the size of the nanoparticles were found to depend on parameters such as pH, temperature, gold concentration and exposure time to gold ions. In the current study, under normal pH conditions, the characteristic SP absorption band at 528 nm was observed after 6 h in case of fungal mycelium, whereas at pH 11, the absorbance band was blue shifted to 518 nm indicating decreased particle size in Au/fungal mycelium solution respect to normal conditions. In case of media at pH 11, the absorbance band at 527 nm was blue shifted to 518 nm with increasing time indicating decreased particles. Under normal conditions, the entrapment of the gold nanoparticles occurs by electrostatic interaction between the gold nanoparticles and within the surface-bound fungal protein for the protein-capped gold nanoparticles. The extracellular nanoparticles synthesis was due to the interaction between pH-dependent aromatic amino acids and gold ions. The yield and time of formation of GNPs was much reduced under alkaline conditions.

Acknowledgements

The authors are thankful to International Foundation of Science, Sweden for the financial support to carry out this work.

References

1. Krolikowska, A.; Kudelski, A.; Michota, A.; Bukowska, J. *Surf. Sci.* **2003**, *532*, 227.
2. Kumar, A.; Mandal, S.; Selvakannan, P.R.; Parischa, R.; Mandale, A.B.; Sastry, M. *Langmuir* **2003**, *19*, 6277.
3. Chandrasekharan, N.; Kamat, P.V. *J. Phys. Chem B.* **2000**, *104*, 10851.
4. Peto, G.; Molnar, G.L.; Paszti, Z.; Geszti, O.; Beck, A.; Guczi, L. *Mater. Sci. Eng C.* **2002**, *19*, 95.
5. Kowshik, M.; Ashtaputre, S.; Kharrazi, S.; Vogel, W.; Urban, J.; Kulkarni, S.K.; Paknikar, K.M. *Nanotechnology* **2003**, *14*, 95.
6. Sastry, M.; Ahmad, A.; Khan, M.I.; Kumar, R.; Microbial nanoparticle production, in: C.M. Niemeyer, C.A. (Eds.), Mirkin Nanobiotechnology, Wiley-VCH Weinheim., Germany, **2004**, pp. 126–135.
7. Mann, S. Biomimetic materials chemistry, Wiley VCH Publishers, New York, **1996**.
8. Nair, B.; Pradeep, T. *Crystal Growth Des.* **2002**, *2*,293.
9. Husseiny, M.I.; El-Aziz, M.A.; Badr, Y.; Mahmoud, M.A. *Spectrochim. Acta A: Mol. Biomol Spectrosc.* **2007**, *67*, 1003.
10. Sastry, M.; Ahmad, A.; Khan, M.I.; Kumar, R. *Curr. Sci.* **2003**, *85*, 162.
11. Shankar, S.S.; Ahmad, A.; Pasrichaa, R.; Sastry, M. *J. Mater. Chem.* **2003**, *131*, 822.
12. Li, Z.; Chung, S.W.; Nam, J.M.; Ginger, D.S.; Mirkin, C.A. *Angew Chem. Int. Ed.* **2003**, *42*, 2306.
13. Sugunan, A.; Melin, P.; Schnürer, J.; Hilborn, J.G.; Dutta, J. *Adv. Mater.* **2007**, *19*, 77.
14. Sujoy K. D.; Enrico M. *Rev Environ. Sci. Biotechnol.* 2010.
15. Mukherjee, P.; Ahmad, A.; Mandal, D.; Senapati, S.; Sainkar, S.R.; Khan, M.I.; Ramani, R.; Parischa, R.; Kumar, P.A.V.; Alam, M.; Sastry, M.; Kumar, R. *Angew Chem. Int. Ed.* **2001**, *40*, 3585.
16. Mukherjee, P.; Senapati, S.; Mandal, D.; Ahmad, A.; Khan, M.I.; Kumar, R.; Sastry, M. *Chem. Bio. Chem.* **2002**, *3*, 461.
17. Underwood, S.; Mulvaney, P. *Langmuir* **1994**, *10*, 3427.

18. Wood, S.A. *Ore Geol. Rev.* **1996**, *11*, 1.
19. Bhattacharya, S.; Srivastava, A. Proc Indian Acad Sci, Chem Sci, **2003**, *115*, pp. 613.
20. Stoscheck, C.M. *Methods Enzymol*. **1990**, *18*, 250.
21. Selvakannan, P.R.; Mandal, S.; Phadtare, S.; Gole, A.; Pasricha, R.; Adyanthaya, S.D.; Sastry, M. *J. Colloid Interface Sci*. **2004**, *26*, 997.
22. Mandal, S.; Phadtare, S.; Sastry, M. *Current. Appl. Phys.* **2005**, *5*, 118.
23. Si, S.; Mandal, T. K. *Chem. Eur. J.* **2007**, *13*, 3160.
24. Yonezawa, T.; Nomura, T.; Kinoshita, T.; Koumoto, K. *J. Nanosci. Nanotechnol.* **2006**, *6*, 1649.
25. Kuo, P. L.; Chen, W. F. *J. Phys. Chem B.* **2003**, *107*, 11267.
26. Chen, S.; Liu, Y.; Wu, G. *Nanotechnology* **2005,** *16*, 2360.
27. Krimm, S.; Bandekar, J. *Adv. Protein Chem.* **1986**, *38*, 181.
28. Nobuki, M.; Ken-ichi, A. *Thin Solid Films* **1999**, *349*, 115.
29. Author, S. *J. Synthetic Organic Chemistry* **1971**, *29*, 27.
30. Tan, Y.; Wang, Y.; Jiang, L.; Zhu, D. *J. Colloid Interface Sci.* **2002**, *249*, 336.
31. Gardea -Torresdey, J.L.; Tiemann, K.J.; Parsons, J.G.; Gamez, G.; Yacaman, M.J. *Adv. Environ. Res.* **2002**, *6*, 313.

